




Cite this: DOI: 10.1039/d5dt02371h

Inverted ligand fields: a conceptual dilemma for molecular orbital theory

Robert J. Deeth 

Ligand field theory (LFT) is generally formulated either as an application of the linear combination of atomic orbitals (LCAO) molecular orbital (MO) model (LFT-MO) or as freely-parameterised crystal field theory with the global crystal field replaced by the local cellular ligand field (CLF) formalism (LFT-CLF). LFT-MO and LFT-CLF are conceptually and numerically different. These differences are highlighted by the LFT-MO concept of an 'inverted ligand field' (ILF). Using formally low-spin d^8 and d^7 ML_4 complexes, it is demonstrated that the LFT-MO ILF concept does not account for how the structures and reactivities of these systems change as a function of L or formal metal oxidation state. The LFT-MO overlap picture is an incomplete representation of how the sub-shell d electrons in transition metal complexes actually interact with their surroundings. The LFT-CLF picture of d electrons localised on the metal, but sensitive to the topology of the ligand field potential, V_{LF} , is a better model. However, V_{LF} does not invert. Instead, the 'internal redox' chemistry that the ILF concept attempts to rationalise is described via the LFT-CLF *d-level breach*. Conceptually, a d-level breach occurs when the bonding levels get too high or the d levels get too low. The empty d levels are filled and the integrity of the original d^n configuration is compromised. A d-level breach should be abrupt with a significant impact on the geometric and electronic structure. This behaviour is confirmed computationally. The d-level breach is thus a significant descriptor for predicting enhanced ligand electrophilicity while the absence of a breach unambiguously and definitively confirms the d^n configuration and metal oxidation state. In contrast, the %d components of canonical LCAO-type MOs used to invoke an ILF are unreliable descriptors and cannot be used to assign oxidation states. In general, ILFs have little chemical relevance but they are important here since they highlight several conceptual and numerical deficiencies of the theory which has underpinned the LFT-MO picture of TM systems for over 60 years.

Received 3rd October 2025,
Accepted 28th November 2025

DOI: 10.1039/d5dt02371h

rsc.li/dalton

Introduction

Ligand field theory (LFT) is often described as an 'application of molecular orbital (MO) theory'.¹ This was not the view of its pioneers, Griffiths and Orgel, who in 1957² considered both Mulliken's method of molecular orbitals and Bethe's electrostatic crystal field theory (CFT) as expressing only 'certain aspects of a more complete theory' which they called LFT.

Of course, in a *numerical* sense, LFT could never have been considered an application of MO theory. LFT has always focussed on the many-electron, multiplet states associated with d–d spectra and paramagnetism and, in 1957, the software required for an '*ab initio*' MO-based calculation of multiplet states was still decades away. The only way of tackling this complicated quantum-mechanical

problem numerically was *via* the ligand field Hamiltonian shown in eqn (1):

$$h_{LF} = \sum_{i < j}^{N_d} U(i, j) + \sum_i^{N_d} V_{LF}(\mathbf{r}_i) + \zeta \sum_i^{N_d} \mathbf{l}_i \cdot \mathbf{s}_i \quad (1)$$

where $U(i, j)$ represents d–d interelectron repulsion, V_{LF} the ligand field potential, and $\mathbf{l} \cdot \mathbf{s}$ spin–orbit coupling. These three terms act upon a basis set of many-electron microstates for the applicable d^n configuration. Thus, LFT provides a fully-correlated, multi-configurational, relativistic treatment albeit restricted to the spectroscopic and magnetic properties dominated by the d states.

The confusion concerning the nature of LFT is *conceptual*. LFT is simply freely-parametrised crystal field theory (CFT)³ and was enormously successful at rationalising the spectral and magnetic properties of coordination complexes. However, its global parameters failed to describe the local σ and π bonding interactions of interest to chemists. For example, in O_h symmetry, there is only one degree of freedom in the e_g - t_{2g}

Department of Chemistry, University of Warwick, Coventry CV4 7AL, UK.
E-mail: r.j.deeth@warwick.ac.uk



splitting of the d orbitals and hence only one parameter, Δ_{oct} , can be fitted to experiment (Fig. 1). Independent measures of σ and π interactions cannot be extracted. Moreover, the expected correlation between the ligand charge and the magnitude of Δ_{oct} was at odds with the values determined from experimental data. The crystal field model did not explain the spectrochemical series since highly electronegative ligands like F^- generated smaller splittings than neutral ligands like carbon monoxide.

In contrast, Mulliken's linear combination of atomic orbitals (LCAO) MO model separated the σ -type e_g MOs from the

π -type t_{2g} MOs. This provided at least a qualitative rationalisation for the spectrochemical series in terms of π -donor ligands pushing the t_{2g} 'd-type' MOs up and making Δ_{oct} smaller *versus* π -acceptor ligands which push the 'd-type' t_{2g} MOs down and increase Δ_{oct} (Fig. 2, left).

The cellular ligand field (CLF) model, introduced by Deeth and Gerloch in 1986⁴ and formerly referred to as ligand field version of the angular overlap model,^{3,5,6} resolved the same issue within the framework of h_{LF} by reformulating V_{LF} in terms of local, σ - and π -bonding parameters. Thus, by design, the CLF model encapsulates the concept of localised M-L bonding and the spectrochemical series is rationalised in a similar manner to LFT-MO: π donors have positive e_π parameters which tends to reduce Δ_{oct} while π acceptors have negative e_π values which tends to increase the d-orbital splitting (Fig. 2, right).

Both models thus account for the trends observed in the spectrochemical series but, crucially, their conceptual and physical bases are completely different. The MO model has *explicit* bonding with ligand-based orbitals interacting with metal-based orbitals. MO formation depends on their relative phases and overlap. The CLF model has *implicit* bonding where the ligand-field d electrons are presumed to be localised on the metal centre but are able to respond to the topology of the *potential field* arising from the bonding electron density. This potential, which has both non-d metal and ligand components, has shape but no phase.

Consequently, in cases where orbital phase is not an issue, such as the conceptual rationale for the spectrochemical series described above, there is no conflict between LFT-MO and LFT-CLF and they present a similar conceptual picture. However, when LFT-MO relies on orbital phase arguments,

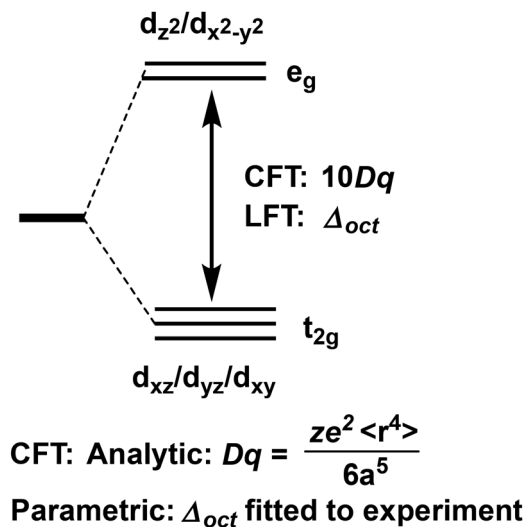


Fig. 1 Octahedral d-orbital splitting diagram. For CFT, the point charges are ze , $\langle r \rangle$ is the averaged d orbital radius and a is the distance between the origin and the point charges.

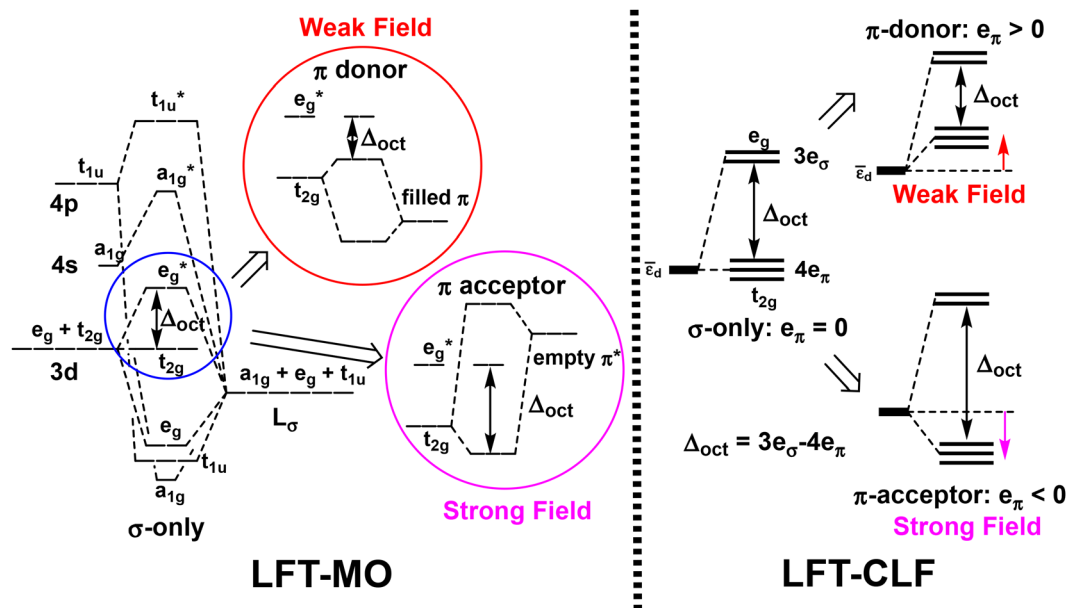


Fig. 2 How local π -donor and π -acceptor bonding effects on the octahedral d-orbital splitting are used to rationalise the spectrochemical series. LFT-MO model (left) and LFT-CLF model (right).



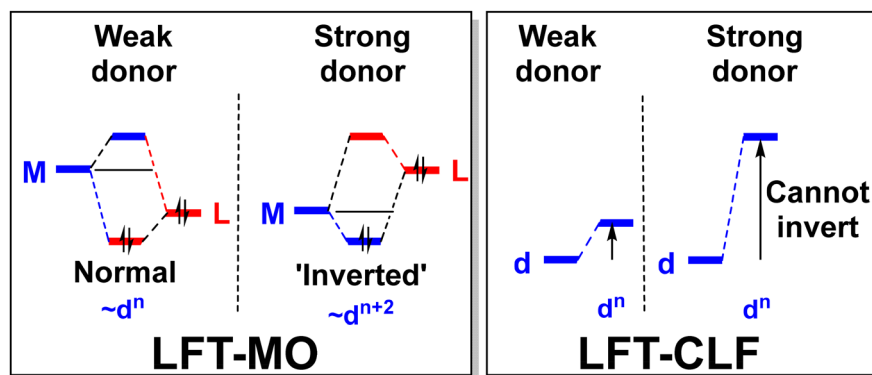


Fig. 3 Left: simplified schematic depiction of the qualitative change in MO composition as a function of the relative energies of the metal and ligand fragment orbitals. Right: effect on ligand-field d orbital of increasing ligand-to-metal donation.

there is invariably a conceptual clash with LFT-CLF.^{7–13} ‘Phase-coupled ligators’ is one such case where an MO-based mechanism generates inconsistencies which manifest in overlap-based approaches such as Schäffer and Jørgensen’s angular overlap model (AOM) but are absent in the CLF picture.¹⁰ The so-called inverted ligand field (ILF) is another such case.

The ILF is an LCAO MO construct involving changes in MO compositions rather than the inversion of the explicit ligand field of the LFT-CLF model which would require a change in field polarity. To highlight this distinction, ILFs will henceforth be referred to as inverted MO sequences (IMOSs).

The composition of MOs depends on the relative energies of the contributing fragment orbitals (Fig. 3, left). In TM systems, if the ligand fragment orbitals lie below the isolated-metal d orbitals, the anti-bonding σ -type MO is mostly metal-based and highest: the ‘ligand field’ is deemed ‘normal’. However, as the energies of the ligand orbitals rise relative to the metal d, the MO compositions change and, ultimately, the bonding MO is mostly metal-based. It is now the lowest energy ‘d’ orbital and the ligand field is deemed to have ‘inverted’. The electrons which started in ligand-based MOs now find themselves in metal-based MOs and the metal is formally reduced.

However, in the LFT-CLF model, the progressive movement of electron density from the ligand to the metal simply leads to a larger CLF parameter value and an increase in the affected d orbital energy (Fig. 3, right). The d-orbital sequence is unaltered and the V_{LF} does not ‘invert’. In addition, if a putative inversion were to occur, the relevant d orbital would have a negative energy (relative to the mean d energy, $\bar{\epsilon}_d$, *vide infra*) and thus the CLF parameter would change sign and the ligand would be deemed an acceptor. Conceptually, achieving this ‘switch’ from ligand-donor to ligand-acceptor behaviour would be abrupt plus this ‘internal electron transfer’ would remove electrons from the bonding levels and place them in the metal d orbitals. The ‘holes’ in the bonding levels would generate Jahn–Teller or pseudo-Jahn–Teller electronic instability and a significant effect on the molecular structure can be anticipated. This contrasts with the LFT-MO picture where it is

argued that the change from normal to inverted is smooth with no apparent effect on structure.¹⁴

The LFT-MO and LFT-CLF conceptual pictures are thus *qualitatively* different and hence their relative performance can be tested numerically. Using a series of formally low-spin d^7 and d^8 complexes, including the archetypal IMOS example $[\text{Cu}(\text{CF}_3)_4]^-$, this paper demonstrates how the IMOS picture, which is based on orbital overlap, is unable to account fully for how the structures and reactivities of these systems change as a function of L or formal metal oxidation state. In contrast, a different conceptual mechanism derived from the potential-based LFT-CLF picture – the d-level breach – is much more successful.

Computational details

All Kohn–Sham (KS) DFT calculations employed the ORCA program system,^{15,16} version 5.0.4. Unless otherwise stated, the standard protocol involved geometry-optimisation using the BP86 functional with def2-TZVP basis sets, Grimme empirical dispersion corrections (keyword D3BJ) and a CPCM solvation field appropriate to ethanol. Where necessary, vibrational analyses were used to confirm local minima, or other stationary points on the potential energy surface, as described in the text. Further details are included in the electronic SI.

The *ab initio* ligand field theory (aiLFT)¹⁷ standard protocol is based on a minimal n electron, 5 orbital (n , 5) active space and employed the DFT-optimised coordinates which, where appropriate, were slightly idealised to the nearest point-group symmetry to aid assignment of the active-space d orbitals. The def2-SVP basis sets were used for all atoms except the metal which retained the def2-TZVP basis.

Briefly, aiLFT is a correlated wavefunction method based on a complete active space self consistent field (CASSCF)¹⁸ treatment of static correlation augmented by an n -electron valence state perturbation (NEVPT2)^{19–22} treatment of dynamic correlation. For a given d^n configuration, use of a minimal active space (ms) comprising 5 orbitals and n electrons generates a



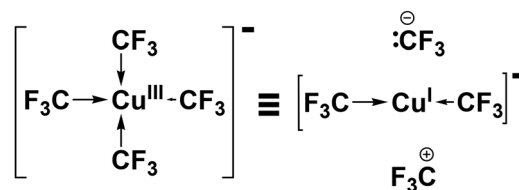
one-to-one mapping between the CASSCF/NEVPT2 energy levels and the relevant Russell–Saunders ligand field multiplets. The CASSCF/NEVPT2 energy differences become a surrogate for the experimental d–d transitions and can be fitted using the conventional ligand-field Hamiltonian (eqn (1)) to generate *ms* aiLFT d-orbital energies and interelectron repulsion parameters in a way akin to, but far more refined than, how Tanabe–Sugano diagrams are used. However, aiLFT has limitations. In general, getting enough, and the correct balance between, static and dynamic correlation is challenging and the minimal active space of aiLFT is relatively small. The analyses in this paper thus rely more on qualitative features than quantitative accuracy.

Results and discussion

$[\text{Cu}(\text{CF}_3)_4]^-$ and other $d^8 \text{Cu}^{\text{III}}$ complexes

The archetypal example of an IMOS is $[\text{Cu}(\text{CF}_3)_4]^-$.^{14,23–32} From the LFT-CLF perspective, this square planar, diamagnetic species exhibits all the hallmarks of a low-spin d^8 species. Hence, the empty, σ -symmetry $d_{x^2-y^2}$ orbital³³ should be highest in energy and the formal OS on copper would be III. Likewise, the standard LFT-MO approach for planar complexes would also place the empty, predominately-metal $d_{x^2-y^2}$ MO at the top of the ‘d-orbital stack’ (Fig. 4, left).

In contrast, Snyder’s³² *ab initio* Hartree–Fock and MP2 calculations on $[\text{Cu}(\text{CF}_3)_4]^-$ yielded Cu 3d populations much closer to 10 than 8. He therefore reformulated the complex as ‘a normal cuprate $[\text{CF}_3\text{–Cu–CF}_3]^-$ in which the copper is



Snyder, 1995

Fig. 5 Formal structural diagrams for $[\text{Cu}(\text{CF}_3)_4]^-$. Left: classical Werner-type structure involving four dative Cu–C bonds from anionic CF_3^- ligands; Right: Snyder’s formulation³² comprising a linear $d^{10} [\text{Cu}^{\text{I}}(\text{CF}_3)_2]^-$ fragment plus nucleophilic CF_3^- and electrophilic CF_3^+ groups.

further coordinated to a trifluoromethyl anion and cation” (Fig. 5).

IMOSs and their implications for the assignment of formal metal d^n numbers and OS became a popular, if somewhat contentious, issue.^{13,14,23,24,26,31,34,35} As described in the seminal review by Hoffmann *et al.*,³¹ the IMOS is a widespread feature of LCAO-type methods including KS DFT. It has also enjoyed strong support from techniques such as X-ray absorption spectroscopy (XAS) to the extent that the ‘experimental’ Cu 3d percentage in the acceptor orbital of nominally Cu^{III} species, including $[\text{Cu}(\text{CF}_3)_4]^-$, is so low that the $d^8 \text{Cu}^{\text{III}}$ formulation has been suggested to be largely mythical³⁵ although this assignment for $[\text{Cu}(\text{CF}_3)_4]^-$ is contradicted by Geoghegan *et al.*²⁷ who favour the $d^8 \text{Cu}^{\text{III}}$ formulation based on a combination of XAS and valence-to-core X-ray emission spectroscopy (VtC XES) data.

However, while interpretations of spectroscopic data may vary, a significant feature of the conceptual LFT-MO picture of 16-electron planar complexes is that an IMOS is not associated with any effect on the structure. Thus, according to the AOM³⁶ analysis presented by Walroth *et al.*¹⁴ (Fig. 6), a stable, square-planar structure is suggested irrespective of the d count (Fig. 6). The MO diagrams of Fig. 4 support this view. The ‘normal’ and ‘inverted’ forms are unremarkable. Thus, LFT-MO predicts that *all* low-spin 16-electron species should be planar irrespective of whether they also have an IMOS or not.

This assertion can be tested numerically. The need to compute reliable structures precludes the strategy adopted by Hoffmann *et al.*³¹ who sought to develop model IMOS systems mainly by manipulating the ligand EHMO H_{ii} parameters. Instead, explicit-electron, KS DFT optimisations were carried out for the series $[\text{CuL}_4]^-$ where the ligand is varied $L = \text{F}, \text{OH}, \text{NH}_2, \text{CH}_3, \text{BH}_2, \text{BeH}$ and Li to mimic the change from the extreme nucleophilicity of F^- to the extreme electrophilicity of Li^- . KS DFT is exceptionally consistent at generating accurate structures of metal complexes and many functionals could be used including BP86^{37,38} providing the basis sets are at least double- ζ quality and that an appropriate dispersion correction and a solvation field are included.

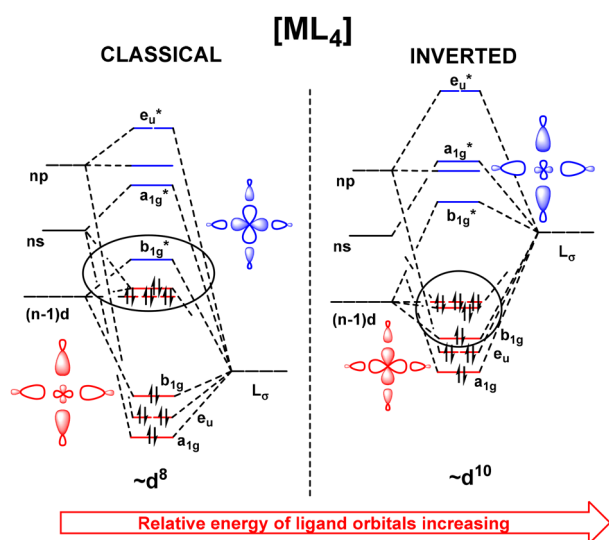


Fig. 4 Qualitative MO energy level diagrams for 16-electron, planar ML_4 species. Left: the ‘classical’, ligand field picture where the ligand orbitals lie below the metal d and the anti-bonding b_{1g} MO is metal centred. Right: the MO compositions invert when the ligand orbital energies are above the d orbitals and the anti-bonding b_{1g} MO is ligand centred. Only orbitals with σ -bonding character are labelled. The nominal d orbitals and electrons are circled.



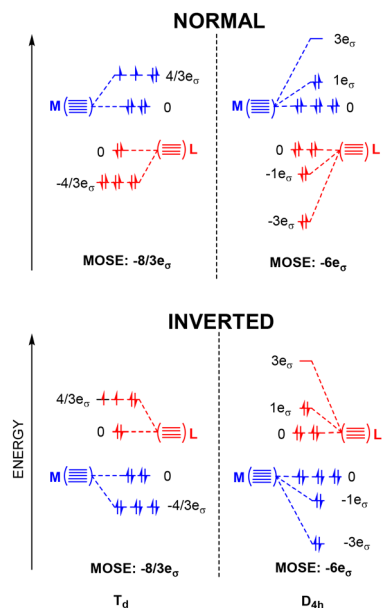


Fig. 6 AOM analysis for σ -only ML_4 systems with 'normal' (top) and inverted (bottom) d-orbital sequences (inverted part after Fig. 3 of ref. 14). Ligand levels in red and d levels in blue. MOSE = molecular orbital stabilisation energy.

Since angle-bending potentials are relatively low,³⁹ metal complexes are quite 'plastic' and the optimised structures are sensitive to subtle electronic effects. The BP86 results are shown in Fig. 7.

There is an abrupt change of structure at $L = BeH$ with distorted structures for $[Cu(BeH)_4]^-$ and $[CuLi_4]^-$. All the other systems, including $[Cu(CH_3)_4]^-$ which, like its CF_3 analogue, has an IMOS, have square planar ground states consistent with low-spin d^8 Cu^{III} . Taken at face value, Fig. 7 demonstrates that the qualitative expectations of LFT-MO are *not met* although sceptics may point to the small energy differences between the optimised local minimum and the planar excited state or query whether the manner of the distortion, or at what point it occurs, is method dependent. To test the latter proposition, B3LYP and TPSSH calculations were carried out. As described in the SI, the hybrid functional results agree with the BP86-based protocol in terms of where the abrupt change occurs. However, the pseudo-Jahn-Teller nature of *breached* systems can present multiple, finely-balanced distortion pathways and the end results may differ. Importantly, though, the issue here is whether an abrupt change in structure happens *at all*. For the moment, therefore, let us proceed on the basis that the geometry change is a real effect and explore how it manifests in the LFT-CLF model and what the further consequences for LFT-MO might be.

The LFT-CLF d-level breach: the conceptual picture

As detailed in the definitive formulation of ligand field theory by Gerloch, Harding and Woolley,³ the LFT-CLF formalism conceives a set of sub-valence-shell $(n-1)d$ electrons localised on the metal. This picture has also been described by

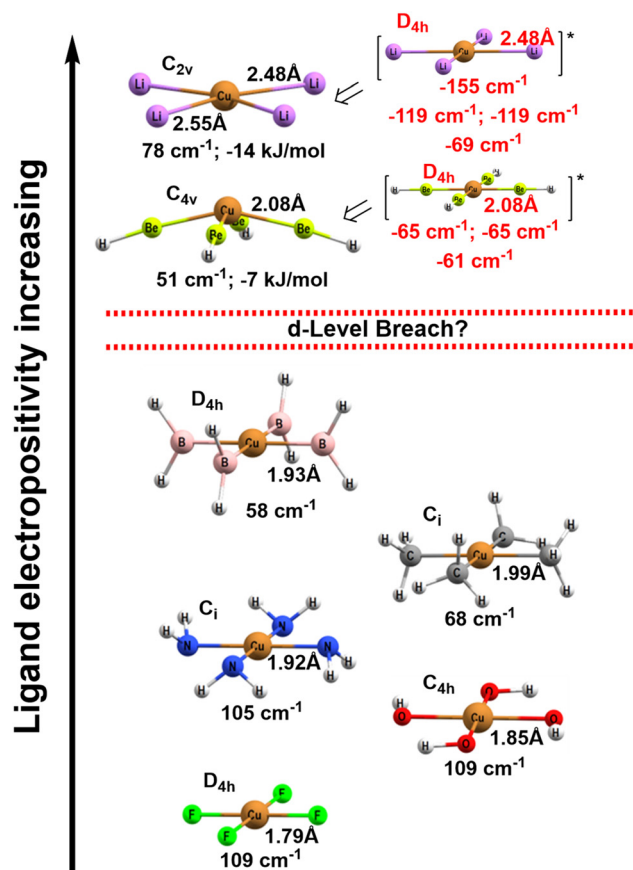


Fig. 7 KS DFT-optimised structures of $[CuL_4]^-$ complexes, $L = F, OH, NH_2, CH_3, BH_2, BeH, Li$ using the standard BP86 protocol. The Cu-L bond lengths and selected vibrational mode energies are included. The lowest energy mode for local minima is shown in black. For $[Cu(BeH)_4]^-$ and $[CuLi_4]^-$, the energy difference between the D_{4h} structure and the actual minimum is also shown. For non-minima, all the calculated imaginary modes are shown in red. Further details are in the SI.

Kaupp.⁴⁰ The $(n-1)d$ orbitals have similar radial properties to the $(n-1)s^2(n-1)p^6$ 'core' and there is strong Pauli repulsion of the bonding electron density. Thus, they overlap poorly with ligand orbitals and can be taken to make no significant contribution to M-L bond formation. However, the 'ligand field' d electrons can still respond to the potential field generated by all the other electrons (and the nuclei) which has a big effect on the properties dominated by the d states. This 'in-complex' viewpoint establishes the reference energy of the ligand-field d levels and is quite different to the zero-overlap, infinite-separation reference in LCAO MO theory.

The most important effects of the ligand-field potential come from the spatially and energetically nearest sources – *i.e.* the electron density localised in the M-L bonds. Conceptually, if the potential from the bonding electrons is below that of the lowest, empty d orbital, the integrity of the d^n configuration is maintained. However, if the bonding level rises above one or more empty d orbitals, or empty d orbitals descend below the bonding level, those d levels are 'breached', filled, and the d^n configuration is compromised. Fig. 8 presents a simplified rep-

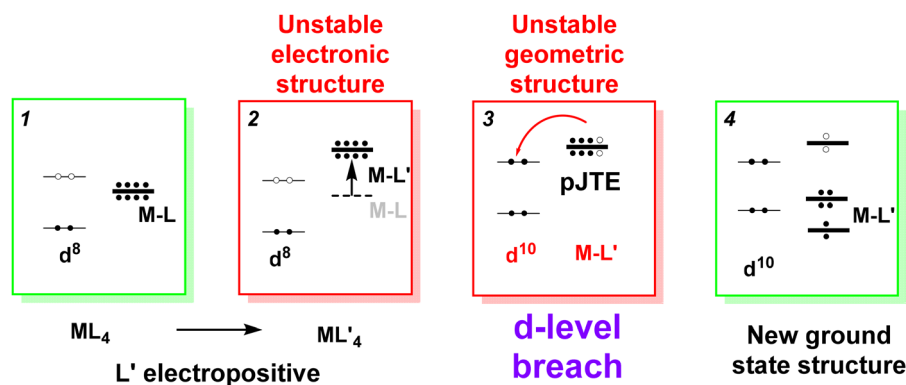


Fig. 8 A simplified, schematic representation of the d-level breach concept for a planar ML_4 system showing the effect of the bonding potential rising above the empty d level. Only the top two d orbitals are shown.

representation of the first 'd-level breach' scenario for a low-spin d^8 ML_4 system, where relatively nucleophilic L is replaced by relatively electropositive L' .

As ligand electropositivity rises, the bonding potential rises, the field strength increases and the d-orbital splitting increases. At some stage, at the prevailing geometry, the bonding potential overwhelms the d orbitals. The left-most panel of Fig. 8 represents the situation just prior to a d-level breach: the bonding potential in ML_4 is high but still lower than that of the empty d level and the d^8 configuration retains its integrity. Replacing L with L' raises the bonding potential above the empty d level generating an unstable electronic state (Fig. 8, panel 2). Electrons 'jump' from the bonding levels to fill the lower-lying empty d orbital thus 'breaching' the d^8 configuration and generating a d^{10} metal centre plus two 'holes' in the bonding levels. Since the latter are degenerate in a square planar environment – they are akin to but different from Pauling hybrids – a pseudo Jahn–Teller effect (pJTE) results and the geometry is unstable (Fig. 8, panel 3). Hence, the complex distorts to re-establish a stable ground state structure with a formally reduced metal centre.

The second scenario where metal oxidation results in the empty d level falling below the bonding potential is basically the same mechanism.

The proposed d-level breach concept is an abrupt internal redox process – either the bonding potential is low enough for the integrity of the original d^n configuration to be maintained or it is so high that the d^n configuration is compromised. In the latter case, punching holes in the bonding potential can be expected to have structural consequences. The geometries in Fig. 7 suggest that only $[Cu(BeH)_4]^-$ and $[CuLi_4]^-$ are breached. Since the IMOS criterion of less than 50% 3d character in the acceptor σ -type MO is met already at $[Cu(CH_3)_4]^-$, the d-level breach structural threshold is clearly higher than the IMOS requirement. This seems reasonable since the empty d orbital which we are trying to breach with a rising bonding potential is being progressively elevated by that approaching potential. This either/or feature of the d^n configuration integrity also echoes the 'winner takes all' oxidation state localised orbitals method of Gimferrer *et al.*²⁸

The d-level breach: numerical analysis of the integrity of the d^n configuration

A significant aspect of the LFT-CLF formalism is the central role of the d^n configuration. This must be assigned at the outset to generate the necessary multiplet states. Hence, in ligand field theory, the d^n configuration has always been *well defined* and, therefore, so too, the associated *formal oxidation state*. This is in contrast to LCAO MO theory, simple or otherwise, where neither the d^n configuration nor the metal oxidation state are well defined and population analyses and MO compositions are method and basis-set dependent. The %d component of a canonical MO is an unreliable descriptor for assigning d^n numbers and formal oxidation states (*vide infra*).

Beyond the breach threshold, the d^n configuration will be compromised and no longer applicable. Moreover, if the 'new' configuration is not an open d shell, the CLF picture may still be valid but this cannot be tested using a model based on h_{LF} . The extension of the conceptual LFT-CLF model to breached systems, as well as formally d^0 and d^{10} systems in general, is beyond the scope of the present manuscript. However, for those d^1 through d^9 systems which fall within the ligand field regime, a successful ms aiLFT^{17,41–43} calculation provides a 'first principles' test of the integrity of the d^n configuration. In the LFT-CLF picture, therefore, the d^n configuration is much more than the 'useful heuristic' suggested by Norman and Pringle.⁴⁴ We will return to this issue in a future publication.

Meanwhile, for the systems shown in Fig. 7, the d^8 aiLFT calculations converge for the square planar systems $[CuF_4]^-$, $[Cu(OH)_4]^-$, $[Cu(NH_2)_4]^-$ and $[Cu(CH_3)_4]^-$ and fail for the distorted systems $[Cu(BeH)_4]^-$ and $[CuLi_4]^-$ (see SI for further details). Interestingly, the model IMOS system, $[Rh(AlMe)_4]^+$, (Fig. 9) which, according to Hoffmann *et al.*,³¹ has an electronic structure consistent with a formally d^{10} Rh^{-1} system, also has a geometrical structure similar to $[Cu(BeH)_4]^-$ consistent with *both* systems having d-level breaches. This conclusion is further supported by the failure of the d^8 ms aiLFT CASSCF step to converge on five suitable active space d orbitals for $[Rh(AlMe)_4]^+$ (see SI).

The CASSCF step for $[Cu(BH_2)_4]^-$ fails too with the CASSCF converging onto three d, one s and one p instead of five mostly



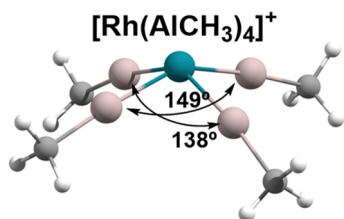


Fig. 9 Model IMOS system proposed by Hoffmann *et al.*³¹ The distorted structure and the failure of the CASSCF step in the ms aiLFT calculation confirm this system also has a d-level breach (see SI.).

d orbitals (see SI), but, given the square-planar structure predicted by DFT, the aiLFT failure is attributed to the shortcomings of the ms aiLFT active space rather than any change in the d⁸ Cu^{III} LFT-CLF picture. Moreover, the central issue is here not the precise point at which the geometry changes abruptly but the fact that there is an abrupt change *at all*. Meanwhile, the aiLFT developers are addressing the limitations of the minimal active space⁴⁵ but a molecular version of the code is not yet available. For the moment, therefore, the presence or absence of a d-level breach is indicated if *both* the dⁿ integrity, as assessed by ms aiLFT, *and* the DFT structure are in accord. If not, then the structural evidence may be more significant.

The effect of a d-level breach on reactivity: [Cu(CF₃)₄][−] vs. Cu(CF₃)₄

The other way to induce a d-level breach is to lower the metal d levels. The relatively low d_{xy} contribution in the active space orbital for D_{2d} symmetric [Cu(CF₃)₄][−] (60.5%) suggests that it is probably near the d-level breach threshold and one could speculate that a further one-electron oxidation to give the formally Cu^{IV} analogue would definitely result in a breach since (i) the higher, formal OS will lower the metal d orbitals and (ii) the low-spin, d⁷ configuration generates a ‘hole’ in one of the low-lying occupied d orbitals which is already closer, and thus more ‘exposed’, to the bonding potential. This prediction contrasts with that derived from the MO diagrams in Fig. 4 which indicate that oxidising [Cu(CF₃)₄][−] simply removes a non-bonding electron.

Optimisation of Cu(CF₃)₄ gives a geometry which is distorted from the approximately planar first-order saddle point of D_{2d} symmetry to a more see-saw structure (Fig. 10, top) of C_{2v} symmetry while the d⁷ ms aiLFT calculation does not generate a suitable set of active space d orbitals and the aiLFT transformation fails. However, in this case, the structure is not definitive support for a d-level breach since a distortion would also result from removing an electron from the degenerate (in D_{2d}) d_{xz}/d_{yz} orbitals thus generating a Jahn–Teller-active ²E state. This occurs for the isoelectronic Ni^{III} analogue where both D_{2d} and see-saw C_{2v} are local minima on the BP86 energy surface (Fig. 10, middle and bottom and SI) with the latter lower in energy by about 10 kcal mol^{−1}. The d⁸ Ni^{II} analogue has the same structure as the Cu^{III} analogue. Significantly, the

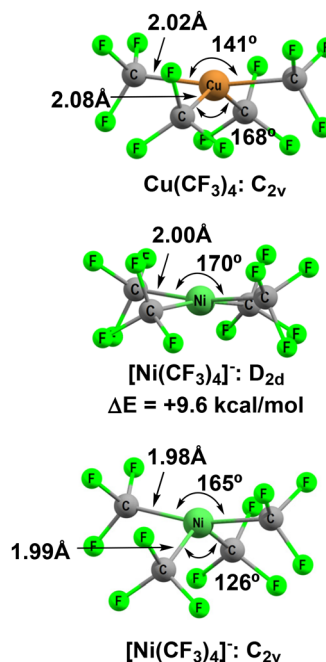


Fig. 10 DFT-optimised local minima for Cu(CF₃)₄ and its isoelectronic nickel analogue [Ni(CF₃)₄][−]. Cartesian coordinates and energies are given in the SI.

d⁷ Ni^{III} and d⁸ Ni^{II} ms aiLFT calculations succeed (see SI) which confirms that the different behaviours of Cu(CF₃)₄ versus [Cu(CF₃)₄][−] are due to the change in oxidation state and therefore that the formally Cu^{IV} system has a d-level breach. This provides an ideal opportunity to compare the IMOS and d-level breach concepts since all four complexes have IMOSs but only Cu(CF₃)₄ has a d-level breach.

Reaction with a nucleophile. Snyder's original formulation of [Cu(CF₃)₄][−] included an electrophilic CF₃⁺ cation (Fig. 5, right)³² which implies substantial electrophilic character.^{24,25,30,31,46} Hoffmann *et al.*³¹ computed the S_N2 reaction energetics between [Cu(CF₃)₄][−] and nucleophiles PH₃ and F[−] (see Fig. 11). The latter gave an exergonic process (ΔG = −29 kcal mol^{−1}) but with a substantial barrier of

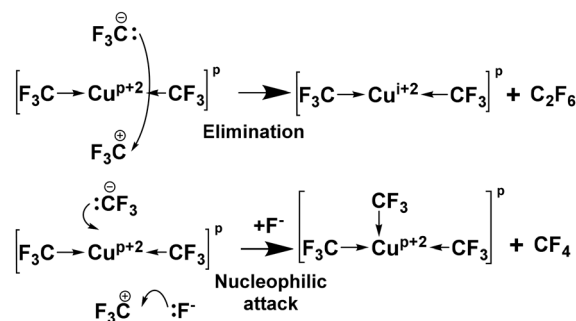


Fig. 11 Reaction schemes for elimination of C₂F₆ (top) and nucleophilic attack by F[−] (bottom) for [Cu(CF₃)₄]^p systems, p = −1, 0 based on Snyder's formulation.



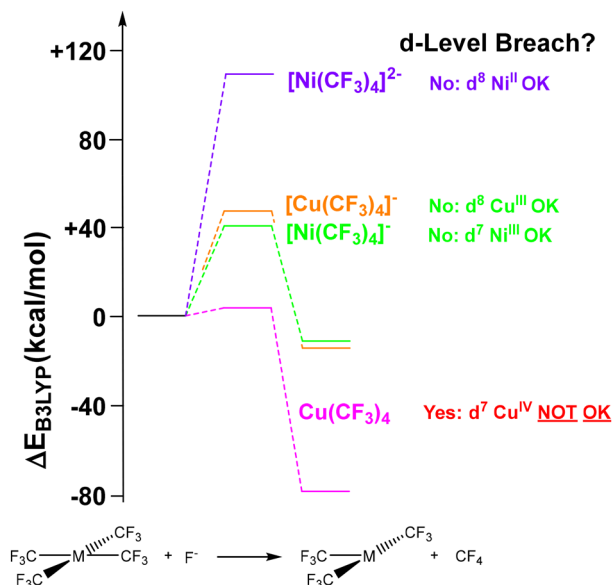


Fig. 12 Calculated reaction profiles for $[\text{M}(\text{CF}_3)_4]^p$ ($\text{M}/p = \text{Cu}/-1, \text{Cu}/0, \text{Ni}/-1, \text{Ni}/-2$) reacting with F^- . Geometries and frequencies were computed using the standard BP86 DFT protocol with B3LYP electronic energies. Further details are in the ESI.

+56 kcal mol⁻¹. The presence of an IMOS in $[\text{Cu}(\text{CF}_3)_4]^-$ is apparently not accompanied by enhanced reactivity. For consistency, these calculations were repeated here using a consistent protocol and then extended to include ‘d⁷’, $\text{Cu}(\text{CF}_3)_4$, d⁷ $[\text{Ni}^{\text{III}}(\text{CF}_3)_4]^-$ and d⁸ $[\text{Ni}^{\text{II}}(\text{CF}_3)_4]^{2-}$.

The results for the four complexes reacting with F^- are shown in Fig. 12.

Clearly, the most telling feature is that a low barrier is only calculated for the system which has a d-level breach. Once again, the presence of an IMOS is unimportant while the presence of a d-level breach is highly significant.

Reductive elimination. Snyder’s formulation of $[\text{Cu}(\text{CF}_3)_4]^-$ might also be expected to facilitate the reductive elimination of C_2F_6 (see Fig. 11). Zimmer *et al.*²³ have studied this computationally but, again, the barrier for $[\text{Cu}(\text{CF}_3)_4]^-$ is significant (51.4 kcal mol⁻¹ by their protocol, 48.5 kcal mol⁻¹ using mine, see SI) which is again consistent with the *absence* of a d-level breach. In contrast, the barrier for the reductive elimination of C_2F_6 from breached $\text{Cu}(\text{CF}_3)_4$ using the standard DFT protocol of this paper is about 40% of the Cu^{III} analogue (19.7 kcal mol⁻¹). The d-level breach has a substantial and specific effect here too.

Reaction pathway of Ni analogues. For comparison, reaction pathways for $[\text{Ni}^{\text{III}}(\text{CF}_3)_4]^-$ and $[\text{Ni}^{\text{II}}(\text{CF}_3)_4]^{2-}$ were also explored. However, starting from the transition state (TS) coordinates for the copper analogues with the same formal d count (Fig. 13), attempts to locate comparable TSs for the reductive elimination of C_2F_6 from the nickel analogues optimised to first-order saddle points corresponding to a different mechanism. As shown in Fig. 14, the nickel complexes appear to prefer to eject a fluoride anion and form a three-coordinate $[\text{Ni}$

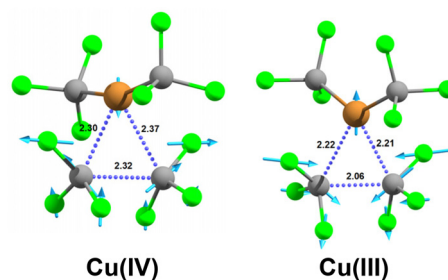


Fig. 13 Optimised transition-state structures for reductive elimination of C_2F_6 from $\text{Cu}(\text{CF}_3)_4$ (left) and $[\text{Cu}(\text{CF}_3)_4]^-$. Selected distances are included as are the weighted displacement vectors of the TS mode. Further details are included in the SI.

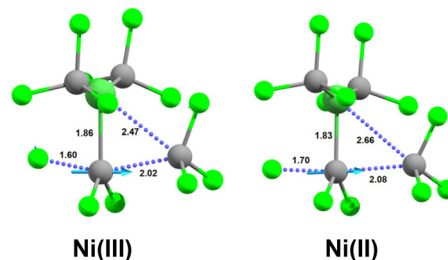


Fig. 14 TS structures, selected interatomic distances (Å) and vectors describing the reaction pathway for $[\text{Ni}^{\text{III}}(\text{CF}_3)_4]^-$ and $[\text{Ni}^{\text{II}}(\text{CF}_3)_4]^{2-}$ (structural and energetic details are included in the SI).

$(\text{CF}_3)_2(\text{CF}_2\text{CF}_3)]^m$ species with the same formal oxidation state as the starting material. Thus, the nickel complexes show none of the electrophilic characteristics anticipated by the IMOS scheme depicted in Fig. 11 but since neither has a d-level breach, no special electrophilic character was to be expected.

The ‘consensus’ view on Cu^{III}

The LFT-CLF formulation of $[\text{Cu}(\text{CF}_3)_4]^-$ as a low-spin d⁸ Cu^{III} system conflicts with the proposed ‘consensus’ view of a d¹⁰ Cu^{I} formulation.¹⁴ Snyder based his assertion on MO calculations but Hoffmann *et al.* make the general claim that “ligand field inversion has been proven spectroscopically”.³¹ And on the basis of XAS supported by KS DFT calculations, DiMucci *et al.* conclude that, with the possible exception of $[\text{CuF}_6]^{3-}$, “physically, d⁸ Cu^{III} does not exist”.³⁵ These assertions require careful qualification.

On the one hand, the notion that d⁸ Cu^{III} does not exist is contradicted both by the results reported above as well as the combined XAS and VtC XES study of Geoghegan *et al.*²⁷ These workers report that the experimental transition energies for the copper N-heterocyclic complexes shown in Fig. 15 are ‘distinctly different’ for each formal oxidation state. The similarities between $[\text{Cu}^{\text{III}}(\text{NHC}_4)]^{3+}$ and $[\text{Cu}(\text{CF}_3)_4]^-$ lead them to formulate the latter also as a d⁸ Cu^{III} complex. In agreement with this proposal, aiLFT calculations for $[\text{Cu}^{\text{II}}(\text{NHC}_2)(\text{NCMe})]^{2+}$, $[\text{Cu}^{\text{III}}(\text{NHC}_2)(\text{NCMe})]^{3+}$ and $[\text{Cu}^{\text{III}}(\text{NHC}_4)]^{3+}$ support d⁹, d⁸ and d⁸ configurations respectively (see SI).



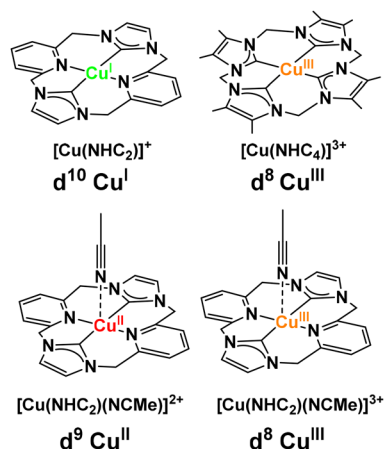


Fig. 15 Structural diagrams for the N-heterocyclic carbene complexes reported in ref. 27. Details of the optimised geometries and aiLFT calculations are in the SI.

On the other hand, the notion that spectroscopy can somehow 'prove' an IMOS needs clarification. As described above, the 'inversion' actually refers to a change in MO composition. An IMOS is therefore a feature of the (fictitious) orbitals of an LCAO MO model, such as the EHMO and Hartree-Fock models or KS DFT. These methods solve a Roothaan-style equation eqn (2), where H is the relevant Hamiltonian matrix, S the overlap matrix, C the MO coefficients and E the MO energies. Thus, if one makes the (subjective) choice to use this type of model to probe the electronic structures of formally Cu^{III} species, then a strong correlation between the %Cu 3d component of the acceptor orbital and the area of the $L_2 + L_3$ XAS absorption is expected. The %Cu 3d contribution for formally Cu^{III} species is generally calculated to be less than 50% so this class of complex satisfies the IMOS condition. However, to then claim that the %Cu 3d contribution to the LUMO of $[Cu(CF_3)_4]^-$ is 35% 'experimentally', as made in Fig. 6 of ref. 35 is invalid. Orbitals are model-dependent and are not observable. Furthermore, the physical significance of the parameters of the LCAO approach – i.e. the MO coefficients – is strictly limited by the nature of the model.

$$(H - ES)C = 0 \quad (2)$$

The goal of the LCAO MO model exemplified in eqn (2) is to generate as low a total energy as possible and the coefficients are optimised accordingly. Hence, the only valid conclusion from the previous work by DiMucci *et al.*³⁵ is that the Löwdin % Cu 3d LUMO contribution is associated with the lowest energy solution of their chosen KS DFT methodology (i.e. B3LYP functional with a CP(PPP) basis set on Cu and ZORA-def2-TZVP(-f) bases on all other atoms). Similar results can be anticipated for other functional/basis set combinations. However, since neither the d^n number nor the metal oxidation state is properly defined in LCAO MO theory *in general*, only the trend is important and the specific %Cu 3d values themselves have no additional significance and are unreliable descriptors for assigning oxidation

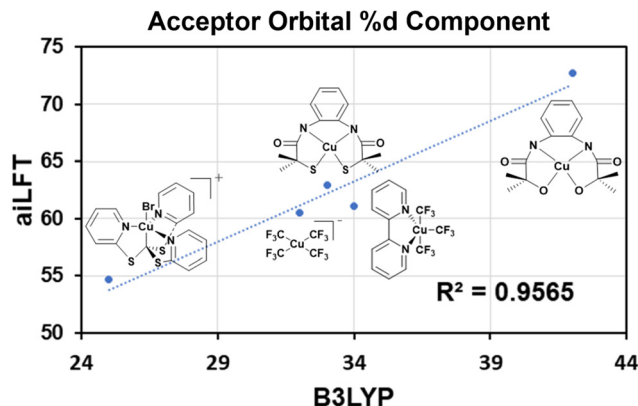


Fig. 16 Correlation between calculated d component (%) in the highest d orbital of the aiLFT active space and the B3LYP acceptor MO for a selection of formally $d^8 Cu^{III}$ complexes. B3LYP data taken from ref. 35. Optimised structures and aiLFT data are given in the SI.

state. The presence (or absence) of an IMOS has no bearing on whether Cu^{III} exists or not.

Of course, comparable constraints apply to the LFT-CLF model. One makes the (subjective) choice to use the LFT-CLF/aiLFT model, and then optimises the CLF parameters/CASSCF coefficients to generate energies of the (fictitious) ligand-field d states which provide the best fit to experimental (or calculated in the case of an aiLFT analysis) d-d spectra and/or magnetic susceptibilities. The crucial difference is that CLF/aiLFT calculations require the d^n configuration to be defined at the start. An acceptable fit/viable active space validates that choice and its associated formal OS. Hence, it is legitimate within the LFT-CLF model to conclude that the successful ms aiLFT calculation for $[Cu(CF_3)_4]^-$ is consistent with its formulation as a low-spin $d^8 Cu^{III}$ complex.

Likewise, the successful aiLFT transformations for $[Cu(CH_3)_4]^-$ and the complexes displayed in Fig. 16, which includes $[Cu(CF_3)_4]^-$, means they can *all* be formulated as d^8 species with 'normal' d-orbital sequences. Significantly, the same *trend* is found for the %d of the highest d orbital from ms aiLFT as from the B3LYP LUMO so both LFT and LCAO MO theory generate the same rank order of changing covalency which is encouraging. However, the components from aiLFT are all greater than 50% so, formally, the criterion for inversion is not even met. From the LFT-CLF perspective, $d^8 Cu^{III}$ is not mythical.³⁵

Finally, and for clarity, the absence of a valid link between the metals' formal oxidation state and the %3d component of a canonical acceptor MO does not imply that the KS DFT electron density distribution is somehow in error. It is simply a question of how this density has been partitioned.

Conclusions

There are two versions of LFT: the 'widely accepted' version which is derived from LCAO MO theory while the less well-



known cellular ligand field version is ultimately derived from crystal field theory. However, there is an important conceptual distinction between the CLF model and CFT. Instead of the crystal field approach which starts with the energy levels of isolated d^n TM ions, the CLF model, as definitively formulated by Gerloch, Harding and Woolley in 1981,³ is rooted in the density functional theorem and starts by considering the division of the *exact*, total electron density of a fully-formed complex into the d-electron component and 'the rest'. And like DFT, the ensuing CLF formalism is also exact in principle but approximate in application. However, if agreement between calculated and experimental data is the yardstick, then the CLF's ability to accurately reproduce the excited-state d-d spectra and ground-state temperature dependence of single crystal paramagnetic anisotropies of metal complexes, which was routinely done already in the 1980s, is impressive testament to the CLF model's veracity.

What seems clear is that the LFT-MO and LFT-CLF models have fundamentally different physical and theoretical foundations. Consequently, the conceptual pictures of how the subvalence-shell d electrons interact with their surroundings are also very different. The LFT-MO picture emphasises *explicit* orbital mixing and the d electrons/orbitals are often strongly delocalised onto the ligands. In contrast, the d electrons in the LFT-CLF picture are localised on the metal and the bonding is treated implicitly.

In the context of so-called inverted ligand fields, or IMOSs as they have been renamed here, each model's predictions of how the structures and reactivities of formally low-spin d^7 and d^8 square-planar ML_4 complexes should vary as a function of L and/or metal oxidation state are qualitatively different.

In the LFT-MO picture for d^8 complexes, the progression from a 'normal' d sequence to an 'inverted' sequence is smooth and progressive. At the normal MO sequence extreme, the orbitals on L are well below the d levels, ligand-metal donation is weak, $d_{x^2-y^2}$ is the highest d level and empty, and the metal is formally d^8 . At the inverted sequence extreme, the orbitals on L are well above the d levels, ligand-metal donation is strong, $d_{x^2-y^2}$ is the lowest d level and filled, and the metal has been formally reduced to d^{10} . Both normal and inverted systems are predicted to have the same geometric structure but the ligands of the inverted form are expected to have enhanced electrophilic character.

In the LFT-CLF conceptual picture, increasing the ligand-to-metal donation simply increases the d-orbital splitting: V_{LF} does not invert. The rising bonding-level potential initially pushes the $d_{x^2-y^2}$ orbital up but the integrity of the d^8 configuration is maintained. Eventually, however, the bonding potential 'swamps' the empty $d_{x^2-y^2}$ orbital causing a d-level breach which formally reduces the metal. The breach is abrupt and generates a (pseudo) Jahn-Teller instability in the bonding levels which leads to a geometric distortion. A breached system is also expected to display enhanced electrophilic reactivity of the ligands.

The combination of DFT geometry optimisations and ms aiLFT d^n integrity tests for low-spin d^7 and d^8 ML_4 complexes

presented here demonstrates that the LFT-MO predictions are not met. For example, there is an abrupt change in structure in the $Cu^{III}L_4$ series while all four complexes, $d^8 [Ni^{II}(CF_3)_4]^{2-}$, $d^7 [Ni^{III}(CF_3)_4]^{2-}$, $d^8 [Cu^{III}(CF_3)_4]^-$ and $d^7 Cu^{IV}(CF_3)_4$, have IMOSs but only $Cu(CF_3)_4$ is breached. The first three complexes have high barriers to reaction with F^- while that for $Cu(CF_3)_4$ is small. The inevitable conclusion is that an IMOS has little chemical relevance. Further theoretical analysis also argues that calculated %Cu 3d values from canonical DFT MOs have little physical significance and cannot be used to assign formal d^n configurations or metal oxidation states since neither quantity is defined in the LCAO MO model. In contrast, the presence of an LFT-CLF d-level breach is highly significant for reactivity while its absence, in conjunction with an appropriate structure, allows for the definitive and unambiguous assignment of the d^n configuration and its associated formal oxidation state.

The results presented here illustrate that the orbital-overlap physics which has underpinned the LFT-MO description of metal-ligand bonding for the past 60 years over-emphasises d-orbital delocalisation/covalency. In contrast, the potential-based CLF model with its localised d electrons is a more realistic representation of how ligand-field d electrons actually interact with their surroundings.

This CLF picture has important conceptual and numerical ramifications for the LFT-MO model which extend beyond the present topic of inverted MO sequences. As will be discussed in a future publication, many of the currently widely accepted concepts of the LFT-MO approach need revision. However, it is important to note that the LFT-CLF model cannot be a universal panacea. There are many situations, such as charge transfer spectroscopy or non-innocent ligands, where h_{LF} simply does not apply but the MO model is useful. The trick will be to acknowledge the strengths and weaknesses of both the CLF and MO approaches and develop a combined conceptual picture which retains their best features whilst avoiding those which lead to conceptual phantoms such as inverted ligand fields.

Conflicts of interest

There are no conflicts to declare.

Data availability

The data that support the findings of this study are available in the supplementary information (SI) of this article. S1: $[CuL_4]^-$ optimised coordinates and aiLFT data for Fig. 7; S2: B3LYP and TPSSH additional calculations; S3: $[Rh(AlMe)_4]^+$ structure and aiLFT results; S4: $[M(CF_3)_4]$ systems; S5: $[M(CF_3)_4]^m$ reactivities: Nucleophilic attack by F^- ; S6: $[Cu(CF_3)_4]^m$ reactivities: Reductive elimination transition states; S7: $[Ni(CF_3)_4]^m F^-$ dissociation; S8: $[Cu(NHC_2)(NCMe)]^m$, $m = +2, +3$ and $[Cu(NHC_4)]^{3+}$ structures and aiLFT results;



S9: Optimised structures and aiLFT data for other Cu^{III} systems shown in Fig. 16.

Supplementary information is available. See DOI: <https://doi.org/10.1039/d5dt02371h>.

Acknowledgements

The author acknowledges the generous software support of Chemical Computing Group and thanks Clark Landis and David Fox for valuable discussions.

References

- M. T. Weller, T. I. Overton, J. P. Rourke and F. A. Armstrong, *Inorganic Chemistry*, Oxford University Press, Oxford, 6th edn, 2018.
- J. S. Griffith and L. E. Orgel, *Q. Rev., Chem. Soc.*, 1957, **11**, 381–393.
- M. Gerloch, J. H. Harding and R. G. Woolley, *Struct. Bonding*, 1981, 1–46.
- R. J. Deeth and M. Gerloch, *J. Chem. Soc., Dalton Trans.*, 1986, 1531–1534.
- M. Gerloch and R. G. Woolley, *Prog. Inorg. Chem.*, 1983, **31**, 371–446.
- M. Gerloch, *Magnetism and Ligand Field Analysis*, Cambridge University Press, Cambridge, 1984.
- R. J. Deeth and M. Gerloch, *Inorg. Chem.*, 1984, **23**, 3846–3853.
- R. J. Deeth, M. J. Duer and M. Gerloch, *Inorg. Chem.*, 1987, **26**, 2573–2578.
- R. J. Deeth, *J. Chem. Soc., Dalton Trans.*, 1993, 1061–1064.
- R. J. Deeth, *Eur. J. Inorg. Chem.*, 2020, 1960–1963.
- R. J. Deeth, *Dalton Trans.*, 2020, **49**, 9641–9650.
- R. J. Deeth, *Eur. J. Inorg. Chem.*, 2022, **2022**, e202100936.
- R. J. Deeth, *Phys. Chem. Chem. Phys.*, 2024, **26**, 18138–18148.
- R. C. Walroth, J. T. Lukens, S. N. MacMillan, K. D. Finkelstein and K. M. Lancaster, *J. Am. Chem. Soc.*, 2016, **138**, 1922–1931.
- F. Neese, *Wiley Interdiscip. Rev.: Comput. Mol. Sci.*, 2018, **8**, e1327.
- F. Neese, *Wiley Interdiscip. Rev.: Comput. Mol. Sci.*, 2012, **2**, 73–78.
- M. Atanasov, D. Ganyushin, K. Sivalingam and F. Neese, in *Molecular Electronic Structures of Transition Metal Complexes II*, ed. D. M. P. Mingos, P. Day and J. P. Dahl, Springer Berlin Heidelberg, Berlin, Heidelberg, 2012, pp. 149–220. DOI: [10.1007/430_2011_57](https://doi.org/10.1007/430_2011_57).
- P. A. Malmqvist and B. O. Roos, *Chem. Phys. Lett.*, 1989, **155**, 189–194.
- C. Angeli, R. Cimiraglia, S. Evangelisti, T. Leininger and J. P. Malrieu, *J. Chem. Phys.*, 2001, **114**, 10252–10264.
- C. Angeli, R. Cimiraglia and J. P. Malrieu, *Chem. Phys. Lett.*, 2001, **350**, 297–305.
- C. Angeli, R. Cimiraglia and J. P. Malrieu, *J. Chem. Phys.*, 2002, **117**, 9138–9153.
- C. Angeli, B. Bories, A. Cavallini and R. Cimiraglia, *J. Chem. Phys.*, 2006, **124**, 054108.
- B. Zimmer, R. W. A. Havenith, J. E. M. N. Klein and K. Koszinowski, *Angew. Chem., Int. Ed.*, 2024, **63**, e202409315.
- I. F. Leach and J. E. M. N. Klein, *ACS Cent. Sci.*, 2024, **10**, 1406–1414.
- P. Alayoglu, T. Chang, C. Yan, Y.-S. Chen and N. P. Mankad, *Angew. Chem., Int. Ed.*, 2023, **62**, e202313744.
- I. F. Leach, R. W. A. Havenith and J. E. M. N. Klein, *Eur. J. Inorg. Chem.*, 2022, **2022**, e202200247.
- B. L. Geoghegan, Y. Liu, S. Peredkov, S. Dechert, F. Meyer, S. DeBeer and G. E. Cutsail III, *J. Am. Chem. Soc.*, 2022, **144**, 2520–2534.
- M. Gimferrer, A. Aldossary, P. Salvador and M. Head-Gordon, *J. Chem. Theory Comput.*, 2021, **18**, 309–322.
- C. Gao, G. Macetti and J. Overgaard, *Inorg. Chem.*, 2019, **58**, 2133–2139.
- M. Baya, D. Joven-Sancho, P. J. Alonso, J. Orduna and B. Menjón, *Angew. Chem., Int. Ed.*, 2019, **58**, 9954–9958.
- R. Hoffmann, S. Alvarez, C. Mealli, A. Falceto, T. J. Cahill, T. Zeng and G. Manca, *Chem. Rev.*, 2016, **116**, 8173–8192.
- J. P. Snyder, *Angew. Chem., Int. Ed. Engl.*, 1995, **34**, 80–81.
- Nomenclature appropriate to D_{4h} symmetry with the X and Y axis coincident with the M–L bonds is used irrespective of the actual the actual point group symmetry.
- M. Kaupp and H. G. von Schnering, *Angew. Chem., Int. Ed. Engl.*, 1995, **34**, 986–986.
- I. M. DiMucci, J. T. Lukens, S. Chatterjee, K. M. Carsch, C. J. Titus, S. J. Lee, D. Nordlund, T. A. Betley, S. N. MacMillan and K. M. Lancaster, *J. Am. Chem. Soc.*, 2019, **141**, 18508–18520.
- C. E. Schäffer and C. K. Jørgensen, *Mol. Phys.*, 1965, **9**, 401.
- A. D. Becke, *Phys. Rev. A*, 1988, **38**, 3098–3100.
- J. P. Perdew, *Phys. Rev. B: Condens. Matter Mater. Phys.*, 1986, **33**, 8822–8824.
- V. J. Burton, R. J. Deeth, C. M. Kemp and P. J. Gilbert, *J. Am. Chem. Soc.*, 1995, **117**, 8407–8415.
- M. Kaupp, *J. Comput. Chem.*, 2007, **28**, 320–325.
- L. Lang, M. Atanasov and F. Neese, *J. Phys. Chem. A*, 2020, **124**, 1025–1037.
- F. Neese, M. Atanasov, G. Bistoni, D. Maganas and S. Ye, *J. Am. Chem. Soc.*, 2019, **141**, 2814–2824.
- J. Jung, M. Atanasov and F. Neese, *Inorg. Chem.*, 2017, **56**, 8802–8816.
- N. C. Norman and P. G. Pringle, *Chemistry*, 2023, **5**, 2630–2656.
- S. V. Rao, D. Maganas, K. Sivalingam, M. Atanasov and F. Neese, *Inorg. Chem.*, 2024, **63**, 24672–24684.
- D. Joven-Sancho, A. Echeverri, N. Saffon-Merceron, J. Contreras-García and N. Nebra, *Angew. Chem., Int. Ed.*, 2024, **63**, e202319412.

